Eur. Phys. J. Plus (2020) 135:665
https://doi.org/10.1140/epjp/s13360-020-00669-1

THE EUROPEAN PHYSICAL JOURNAL PLUS

Regular Article

Simple FFH pilot experiment model based on DTT-like machine

F. Panza[1,a], **I. Balog**[1], **A. Cemmi**[1], **I. Di Sarcina**[1], **F. Filippi**[1], **E. Mansi**[1], **F. P. Orsitto**[2], **M. Osipenko**[3], **G. Ricco**[3,4], **M. Ripani**[3,4], **M. Ciotti**[1]

[1] ENEA Casaccia, S. Maria di Galeria, Rome, Italy
[2] Consorzio CREATE Università di Napoli Federico II, Naples, Italy
[3] Istituto Nazionale di Fisica Nucleare - Sezione di Genova, Genoa, Italy
[4] *Present Address*: Centro Fermi - Museo Storico della Fisica e Centro Studi e Ricerche "Enrico Fermi", Rome, Italy

Received: 19 December 2019 / Accepted: 3 August 2020 / Published online: 18 August 2020

Abstract The global need for energy in the world is constantly increasing. Critical fission reactors have proved great efficiency in the energy production, but the fear of nuclear wastes and accidents due to an uncontrolled chain reaction makes these unpleasant to public. More safe fusion reactors, on the opposite, have low efficiency. Hybrid reactors capable of using the advantages of both are studied, but not yet developed. In this paper, a simple fusion–fission pilot experiment model has been developed. A Tokamak with the same characteristics of DTT (Divertor Tokamak Test facility) has been considered as a reference machine for the fusion component. The fusion system has been coupled with a relatively simple low-power fission blanket configured into three different modes by using different fuels and materials. This model could be useful in order to investigate the properties of the fusion–fission hybrid coupling from a neutronic point of view.

1 Introduction

A fusion–fission hybrid reactor (FFH) has two main subsystems: a fusion reactor, acting as a neutron source, and a subcritical fission blanket, composed by an assembly of nuclear fuel, acting mainly as a power amplifier. This scheme has the aim to use the large amount of energy produced by the burning of the fission fuel with the low nuclear waste production allowed by the neutron produced in the DD reaction, keeping safe the reactor due to the subcritical working point which allows a better control of the reactor avoiding the uncontrolled melt down of the fission core.

In this context, a pilot experiment could be considered as a relatively low-power FFH, so that the fusion reactor characteristics could be less demanding, because a significant part of the thermal power would be produced by the fission blanket thanks to its amplification properties. This could imply, for example, a higher fusion duty cycle, which is fundamental to reduce the thermal material stress in the fission blanket components, due to the fast thermal power variations.

[a] e-mail: fabio.panza@enea.it (corresponding author)

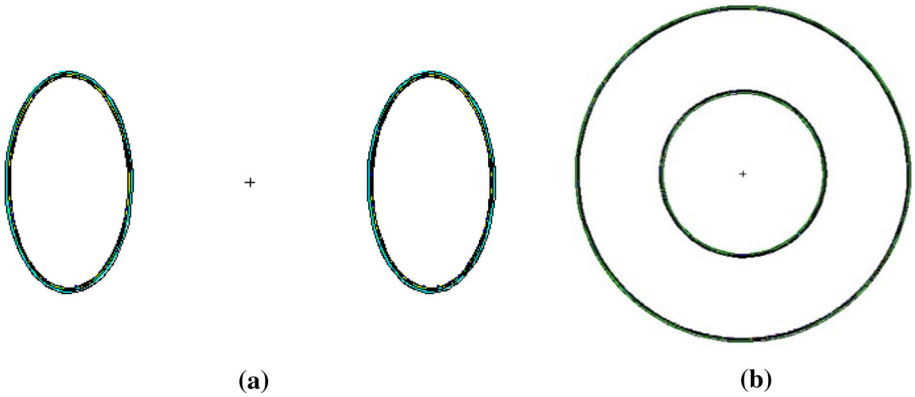

Fig. 1 Side (**a**) and top (**b**) schematic views of DTT tokamak with the relative geometric characteristics

In this work, we considered a tokamak reactor with the same DTT (Divertor Tokamak Test facility) [1] characteristics in terms of materials, geometry and magnetic fields, as a neutron source for three different configurations of subcritical fission blankets: a MOX[1]–lead, a MOX–water and a spent fuel–water system.

The aim of this work is to use the Monte Carlo code MCNP6.1 simulation code [2] with ENDF/B-VII.1 libraries to perform a simple design study regarding the coupling between these two components of a FFH. The study is based on DTT, a fusion machine that has been already designed and whose construction has just started, and a relatively well-known fission subcritical system. The aim of the Monte Carlo simulations is to investigate the main characteristics of such a FFH for a pilot experiment.

2 Fusion system

In order to study a possible hybrid reactor configuration, we have considered as a starting point the parameters of the DTT tokamak which will be built in the ENEA Frascati research center as a divertor test machine supporting ITER project [3].

DTT is a tokamak inducing D–D fusion reactions with the following main characteristics shown in Fig. 1a, b:

- major radius $R = 215$ cm
- minor radius $a = 70$ cm
- aspect ratio $A = 3.1$ ($A = R/a$)
- elongation 1.8
- toroidal field $B = 6$ T
- plasma current $I_p = 6$ MA
- D–D fusion power $P_{fus} = 11$ kW

We have taken the simulated neutron spectrum produced in the DTT machine, and we have analyzed their spectrum after crossing the wall of the machine. The first DTT wall has been simulated by using the following effective material thicknesses as shown in Fig. 2:

- Tungsten: 0.5 cm

[1] MOX: mixed Uranium–Plutonium oxides fuel.

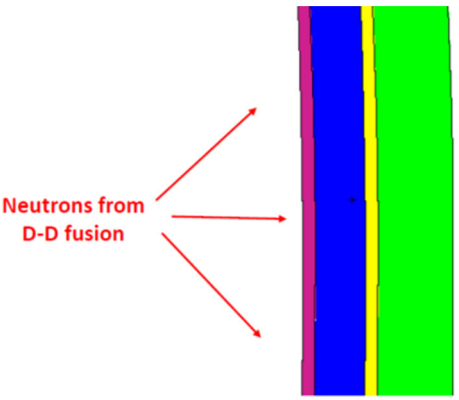

Fig. 2 Effective thicknesses and materials of the first DTT wall: tungsten (purple), copper (blue), water (yellow), steel (green)

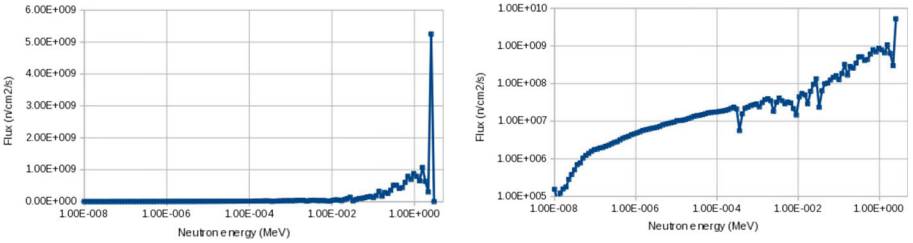

Fig. 3 Log–lin (left) and log–log (right) absolute energy spectrum of neutrons emerging from first DTT wall

- Copper: 2 cm
- Water: 0.5 cm
- Steel: 3 cm

The neutrons emerging from the first wall and entering in the fission blanket have the energy spectrum reported in Fig. 3.

DTT will work with the DD fusion reaction, producing two possible reactions:

- $d + d \rightarrow {}^3\mathrm{He} + n + 3.27$ MeV (50%)
- $d + d \rightarrow {}^3\mathrm{H} + p + 4.03$ MeV (50%)

Since the overall emerging neutron intensity is about 10^{16} n/s, a fusion power of 5 kW is generated by the ${}^3\mathrm{He} + n$ contribution, while a power of 6 kW is produced by the ${}^3\mathrm{H} + p$ contribution. The total fusion power is about 11 kW. Therefore, in the simulations we generated 2.5 MeV neutrons emerging with random direction from the plasma volume, with nominal overall intensity of 10^{16} n/s.

3 Fusion–fission pilot experiment

Starting from the above tokamak characteristics, a subcritical modular fission blanket, driven by neutrons with the energy spectrum shown in Fig. 3, has been studied.

Three different configurations surrounding only a sector of the external section of the torus (Fig. 4) have been considered:

- Solid lead fission blanket fueled with MOX [4] and cooled by water pipes (MOX–lead configuration)

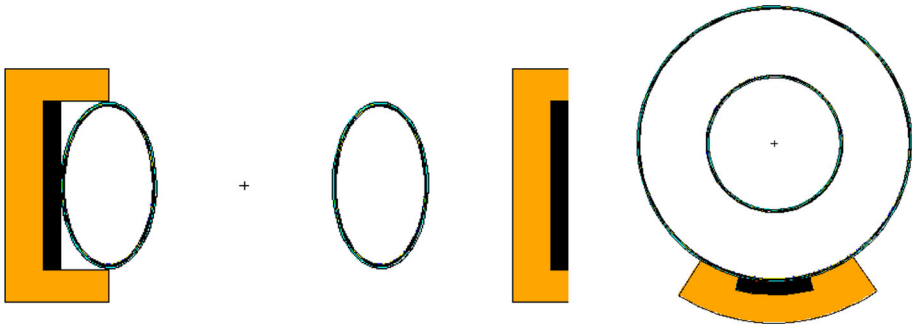

Fig. 4 Side (left) and top (right) schematic views of the fusion–fission hybrid system. The fission core is represented by the black region (fuel rods) and the reflector by the yellow region

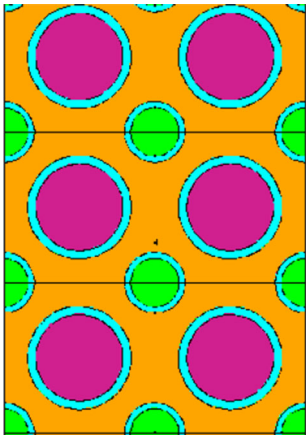

Fig. 5 Core lattice for MOX–lead configuration: MOX fuel in purple, water in green, steel cladding in light blue and lead in yellow

- Water moderated and cooled fission blanket fueled with MOX (MOX–water configuration)
- Water moderated and cooled fission blanket fueled with spent fuel (spent fuel–water configuration)

Each of the previously mentioned FFH configurations has the same conceptual design of the structure reported in Fig. 4. The considered fission blanket materials and thicknesses will be described in detail in the following paragraphs.

The following simulations have been performed by using MCNP6.1 code with ENDF/B-VII.1 libraries. The total number of generated neutrons is 2×10^7, while for the evaluation of the effective multiplication factor, kcode mode with 120 active cycles with 5000 particles per cycle has been used.

3.1 MOX–lead configuration

The fission blanket configuration reported in Fig. 5 [5] is composed by 0.357-cm-radius, 262-cm-high and 0.068-cm steel-clad MOX designed for ALFRED reactor project (Table 1) fuel rods ($m_{\text{fuel}} = 2.5$ ton). The rods are completely embedded in a solid lead matrix. The cooling system is provided by steel water pipes ($R = 0.25$ cm, thickness 0.05 cm). The 25-cm-thick and 150-cm-long fission core is surrounded by 50-cm-thick lead reflector.

Table 1 MOX fuel vector as designed for ALFRED reactor project [4]

Element	Concentration (%)
Uranium	78
Plutonium	22

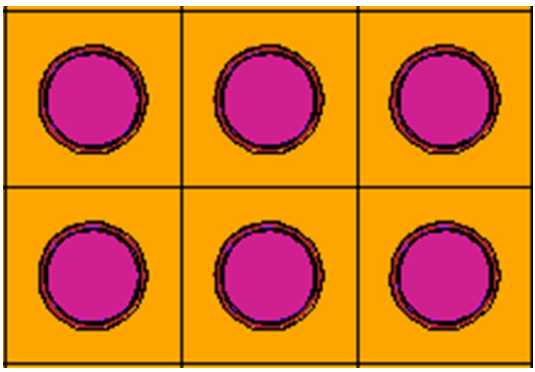

Fig. 6 Core lattice for MOX–water configuration: MOX fuel in purple, water in yellow, Zircaloy cladding in brown

From our simulations, we observed that the effective multiplication factor for this configuration is $k_{\text{eff}} = (0.86072 \pm 0.00079)$ and the generated fission thermal power is $P = (20.595 \pm 0.064)$ kW.

3.2 MOX–water configuration

This fission blanket configuration is formed by 0.45-cm-radius and 262-cm-high 0.068-cm Zircaloy-clad MOX (Table 1) fuel rods ($m_{\text{fuel}} = 0.7$ ton) embedded in water acting both as a neutron moderator and as a coolant as shown in Fig. 6. The fission core of 7 cm thick and 150 cm long is surrounded by a 100-cm-thick graphite reflector.

The effective multiplication factor for this configuration is $k_{\text{eff}} = (0.82689 \pm 0.00100)$, and the generated fission thermal power is $P = (20.825 \pm 0.54)$ kW.

3.3 Spent fuel–water configuration

This fission blanket configuration is formed by 0.45-cm-radius and 262-cm-height 0.068-cm Zircaloy-clad spent fuel (standard PWR 33 GWd/ton after a cooling time of 10 years, Table 2) [6] rods ($m_{\text{fuel}} = 3.7$ ton) embedded in water acting both as a neutron moderator and as a coolant. The core lattice has the same geometry of the MOX–water configuration shown in Fig. 6. The 35-cm-thick and 150-cm-long fission core is surrounded by a 100-cm-thick graphite reflector.

The effective multiplication factor for this configuration is $k_{\text{eff}} = (0.88352 \pm 0.00075)$, and the generated fission thermal power is $P = (20.537 \pm 0.072)$ kW.

Table 2 Spent fuel vector (standard PWR 33 GWd/ton after a cooling time of 10 year)

Element(s)	Concentration (%)
Uranium	95.53
Plutonium	0.83
Minor actinides	0.11
Long-lived fission products	0.19
Medium-lived fission products	0.16
Stable isotopes	3.18

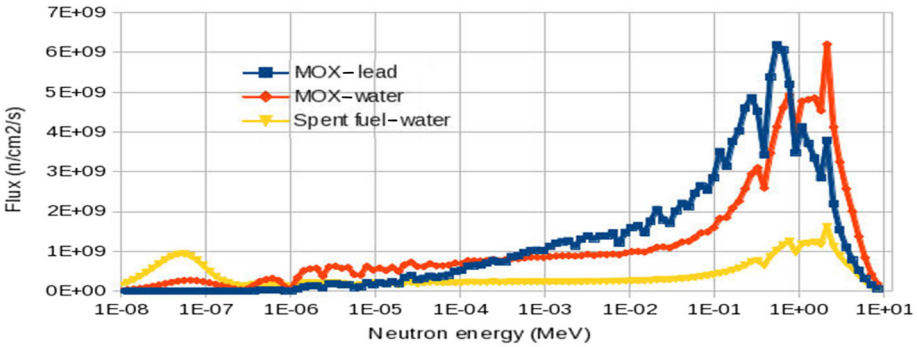

(a)

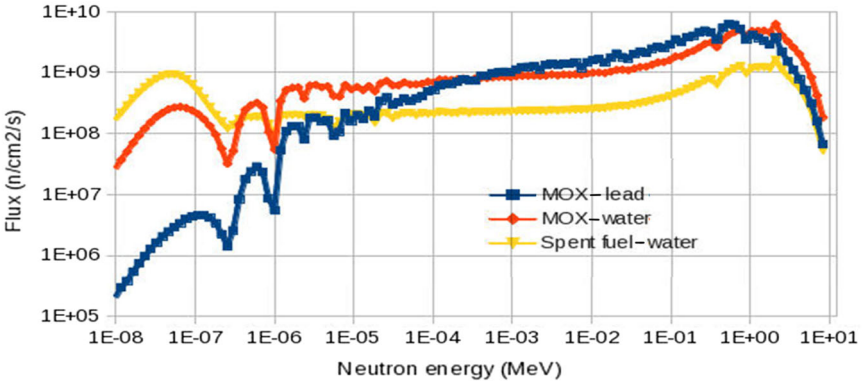

(b)

Fig. 7 Neutron energy distribution (log–lin (**a**) and log–log (**b**)) for MOX–lead configuration (blue line), MOX–water configuration (red line) and spent fuel–water configuration (yellow line)

4 Results

4.1 In-core neutron energy spectra

The energy flux distributions for the three previously described configurations are reported in Fig. 7a, b.

The three considered spectra present different behaviors due to the different characteristics of each configuration. We considered a "fast" fission blanket (MOX–lead), a "quasithermal" system (MOX–water) and a "thermal" system (spent fuel–water).

The previous figures clarify the differences between the three considered configurations: The ratio between the fast flux component (above 0.5 MeV) and the slow component (below 1 eV) can give an idea of the "hardness" of each spectrum. This ratio is higher in the MOX–lead configuration, while it is lower in the MOX–water and in the spent fuel–water configuration because, as expected in a light water moderated core, the slow component is higher with respect to the others as clearly shown in Table 3.

The differences between the "fast" configuration and the others are evident. In particular, the two water moderated configurations present a larger difference in the low-energy region: The MOX–water configuration has a lower thermal region flux with respect to the spent fuel–water configuration that shows an elevated flux intensity in the same energy region. This behavior can be imputed to the higher presence of thermal neutron absorbers in the MOX fuel. Moreover, in both water configurations, the distance between two adjacent fuel rods is not sufficient for a good neutron thermalization. For this reason, the slow flux component for the water moderated configurations is lower with respect to the one in a typical thermal reactor.

4.2 Power amplification factor

In all configurations, the overall power due to the $d + d \rightarrow {}^3\mathrm{He} + n$ reaction is about 5 kW, while the others 6 kW are produced by $d + d \rightarrow {}^3\mathrm{H} + p$ which does not contribute to the fission blanket amplification.

The fission blanket covers only a small portion of the torus surface which is almost 2.4% of the total area. Assuming an isotropic emission from the neutron production channel, the power impinging on the fission blanket is about 0.12 kW.

Since the fission blanket produces a thermal power of about 20 kW, the amplification factor (i.e., the ratio between the fission blanket power and the fusion power) has been evaluated for the overall neutron channel fusion power production and for the part of it impinging on the fission blanket. Those factors are, respectively, 4 and 167. If we consider the total fusion power (11 kW), the amplification factors are 1.82 and 75.76. The amplification factor values show that even if only a sector of the torus surface is covered by the fission blanket it is possible to obtain a good power amplification, in spite of only a part of fusion power being amplified.

5 Sensitivity analysis

A sensitivity analysis by using the previously mentioned models has been performed, and the results obtained by using the data libraries ENDF/B-VII.1 (used in the calculations reported above) and JEFF-3.2 have been compared.

The results of the simulations by using JEFF-3.2 libraries are reported in Table 4.

The ratios between integral flux, power and effective multiplication factor calculated by using ENDF/B-VII.1 end JEFF-3.2 libraries in the three considered configurations are shown in Table 5.

In Figs. 8, 9 and 10 are reported the ratio values between the flux energy distribution (bin per bin) obtained by using ENDF/B-VII.1 end JEFF-3.2 in the three previously mentioned configurations, respectively.

Table 3 Integral flux values, flux percentage below 1 eV (slow component), above 0.5 MeV (fast component), ratio between fast and slow flux components, thermal power and effective multiplication coefficient, k_{eff}, for the three considered configurations obtained by using ENDF/B-VII.1 libraries

Configuration	Integral Φ (n/cm^2/s)	$\Phi < 1$ eV (%)	$\Phi > 0.5$ MeV (%)	$\Phi > 0.5$ MeV/$\Phi < 1$ eV	Power (kW)	k_{eff}
MOX–lead	$(1.456 \pm 0.005) \times 10^{11}$	0.110	37.255	339.901	20.595 ± 0.064	0.86072 ± 0.00079
MOX–water	$(1.393 \pm 0.003) \times 10^{11}$	3.175	45.695	14.394	20.825 ± 0.54	0.82689 ± 0.00100
Spent fuel–water	$(4.816 \pm 0.002) \times 10^{10}$	24.615	34.057	1.384	20.537 ± 0.072	0.88352 ± 0.00075

Table 4 Integral flux values, flux percentage below 1 eV (slow component), above 0.5 MeV (fast component), ratio between fast and slow flux components, thermal power and effective multiplication coefficient for the three considered configurations obtained by using JEFF-3.2 libraries

Configuration	Integral Φ (n/cm^2/s)	Φ <1 eV (%)	Φ >0.5 MeV (%)	Φ >0.5 MeV/Φ <1 eV	Power (kW)	k_{eff}
MOX–lead	$(1.438 \pm 0.005) \times 10^{11}$	0.108	37.380	347.325	20.394 ± 0.063	0.85518 ± 0.00085
MOX–water	$(1.363 \pm 0.003) \times 10^{11}$	3.168	45.791	14.455	20.727 ± 0.052	0.82384 ± 0.00107
Spent fuel–water	$(4.637 \pm 0.002) \times 10^{10}$	24.563	34.014	1.385	19.727 ± 0.065	0.87707 ± 0.00068

Table 5 Ratios between integral flux, power and effective multiplication factor calculated by using ENDF/B-VII.1 and JEFF-3.2 libraries for the three selected configurations

Configuration	R = integral Φ (ENDF)/integral Φ (JEFF)	Power (ENDF)/power (JEFF)	k_{eff} (ENDF)/k_{eff} (JEFF)
MOX–lead	1.011 ± 0.004	1.009 ± 0.004	1.006 ± 0.001
MOX–water	1.022 ± 0.004	1.005 ± 0.004	1.004 ± 0.002
Spent fuel–water	1.039 ± 0.005	1.041 ± 0.005	1.007 ± 0.001

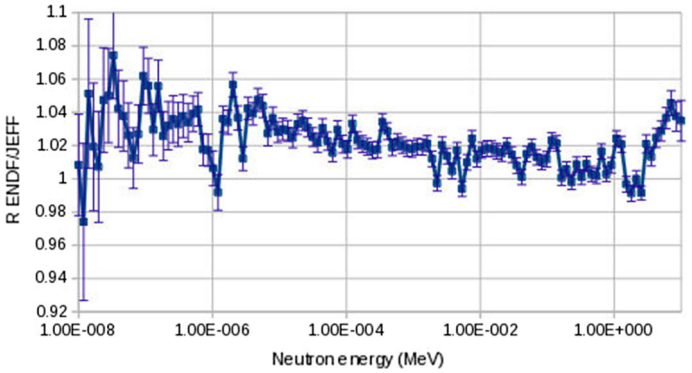

Fig. 8 Ratio between the integral mean fluxes for MOX–lead configuration evaluated by using ENDF/B-VII.1 end JEFF-3.2 libraries

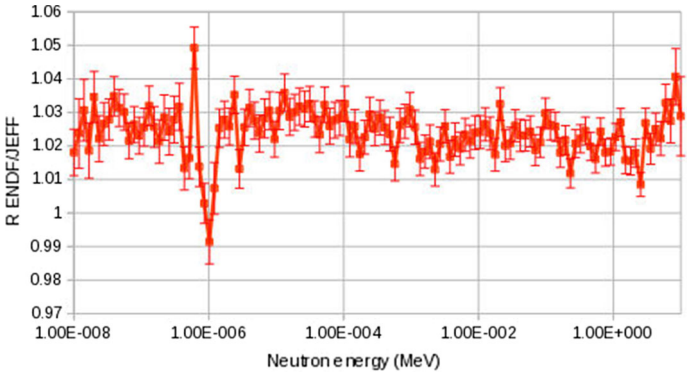

Fig. 9 Ratio between the integral mean fluxes for MOX–water configuration evaluated by using ENDF/B-VII.1 end JEFF-3.2 libraries

As shown in Table 5 and in Figs. 8, 9 and 10, such ratios exhibit in general a small difference from unity. In particular, the ENDF/B-VII.1 results appear systematically higher than JEFF-3.2 ones. However, flux, power and multiplication coefficient differ from each other only by a few percent. Most importantly, such discrepancies do not compromise the large, safe margin to criticality of all three systems.

We observe that ENDF/B-VII.1 libraries give a systematically higher flux than JEFF-3.2 ones. However, the corresponding power and k_{eff} do not show such systematic effect in one direction. Such differences must certainly come from differences in the two cross-sectional

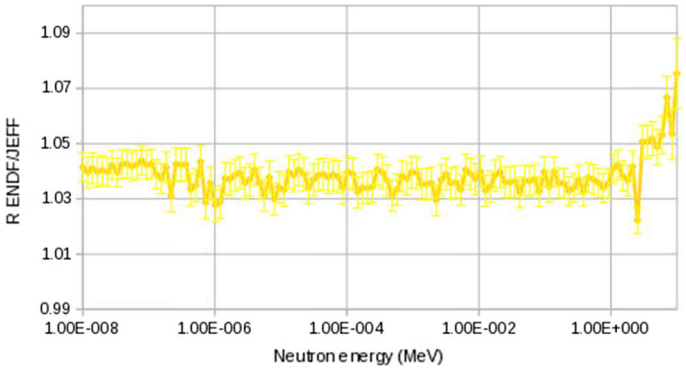

Fig. 10 Ratio between the integral mean fluxes for spent fuel–water configuration evaluated by using ENDF/B-VII.1 end JEFF-3.2 libraries

libraries for various processes and materials, whose detailed analysis would require a separate study.

6 Conclusions

A low-power fusion–fission hybrid pilot experiment based on DTT machine has been studied. The aim of these calculations is to investigate the feasibility of a preliminary hybrid configuration on a fusion machine that represents a typical Tokamak with the presently manageable level of complexity. The subcriticality of the fission part gives the possibility to choose among a large number of fission fuels as shown in our simulations where two representative fuel types have been assumed. Three low-power fission blanket configurations with different kinds of fuels (MOX/spent fuel) have been considered in order to evaluate the effects of different host materials (lead and water) from a neutronic point of view.

The energy amplification factors have been evaluated, and we found them to be about 1.82 if dividing the fission power by the overall fusion power produced and about 75.76 if considering only the power fraction impinging on the fission blanket. We find this to be remarkable, considering that the design is based on a research machine not devoted to energy production.

A sensitivity analysis has been performed by comparing the results obtained by using ENDF/B-VII.1 and JEFF-3.2 libraries. Small differences between flux, power and multiplication coefficient are evident in this comparison. However, they are within a few percent so that the basic features of the systems, in particular their large margin to criticality, are confirmed.

Even though a detailed discussion is beyond the scope of this paper, we believe that a simple pilot experiment, although not trivial in terms of installation and safety aspects, may be designed and practically implemented.

Further studies will be performed in the near future in order to investigate the possibility to obtain a higher amplification factor with the same subcriticality value by optimizing the geometry.

Funding Open access funding provided by Ente per le Nuove Tecnologie, l'Energia e l'Ambiente within the CRUI-CARE Agreement.

References

1. https://www.dtt-project.it/index.php
2. T. Goorley, MCNP6.1.1-Beta Release Notes, LA-UR-14-24680 (2014)
3. https://www.iter.org/
4. Ansaldo Nucleare spa. Private communication
5. F. Panza et al., Ann. Nucl. Energy **109**, 162 (2017)
6. http://www.jaif.or.jp/ja/wnu_si_intro/document/2009/m_salvatores_advanced_nfc.pdf. Accessed 2009